Potential-driven sulfate coordinated active configuration for Electrochemical C-H bond activation

Jui-Hsien Chen[1], You-Chiuan Chu[1], Tong Lin[2], Cheng-Han Tso[1], Guan-Bo Wang[1], Chia-Shuo Hsu[3], Hao Ming Chen[1,3,4] Hsiao-Chien Chen[2,5]*

[1]*Department of Chemistry, National Taiwan University, Taipei 10617, Taiwan*

[2]*Center for Reliability Science and Technologies; Center for Sustainability and Energy Technologies, Chang Gung University, Taoyuan 33302, Taiwan*

[3]*National Synchrotron Radiation Research Center, Hsinchu 30076, Taiwan*

[4]*Center for Emerging Materials and Advanced Devices, National Taiwan University, Taipei 10617, Taiwan*

[5]*Kidney Research Center, Department of Nephrology, Chang Gung Memorial Hospital, Linkou, Taoyuan 33305, Taiwan*

Email: hc_chen@mail.cgu.edu.tw

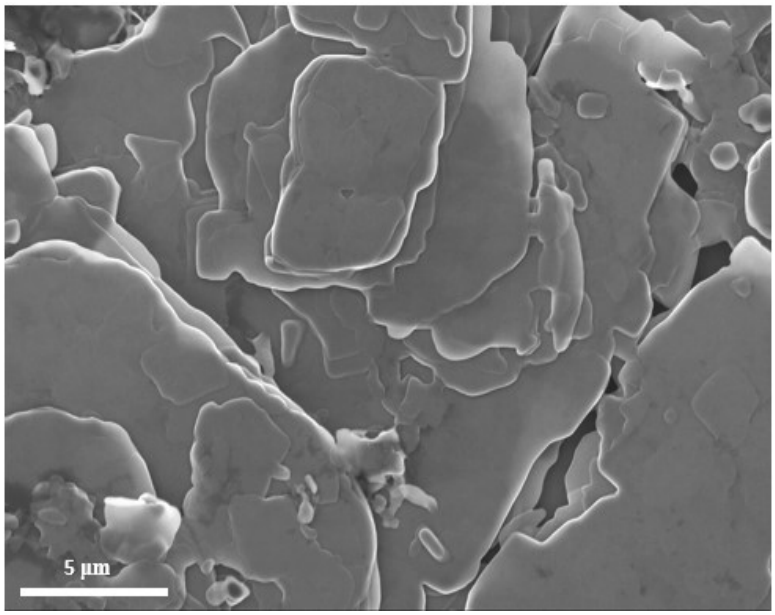

Supplementary Figure S1. SEM image of bulk $VOPO_4 \cdot 2H_2O$.

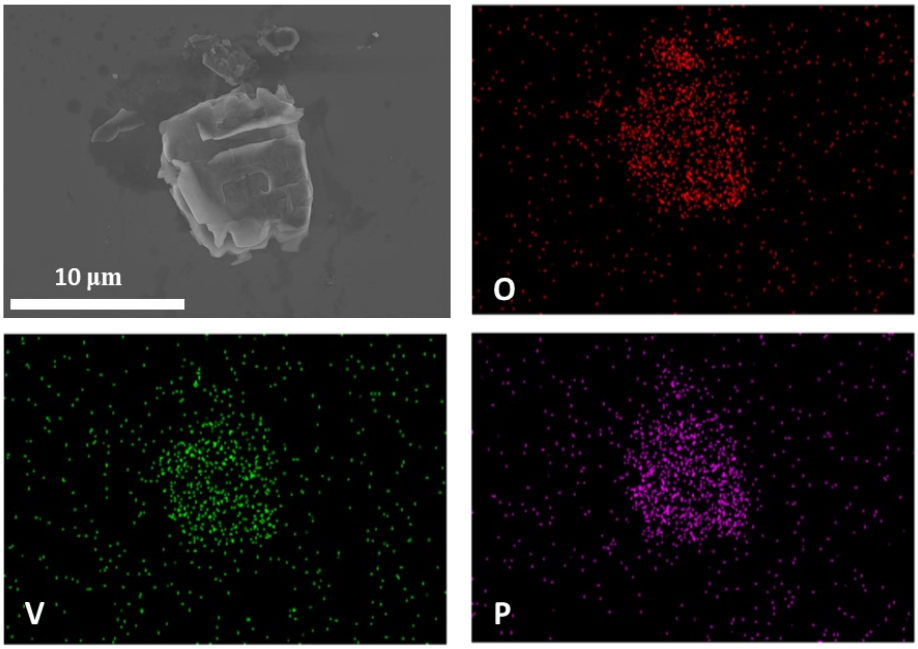

Supplementary Figure S2. EDS image of bulk $VOPO_4 \cdot 2H_2O$.

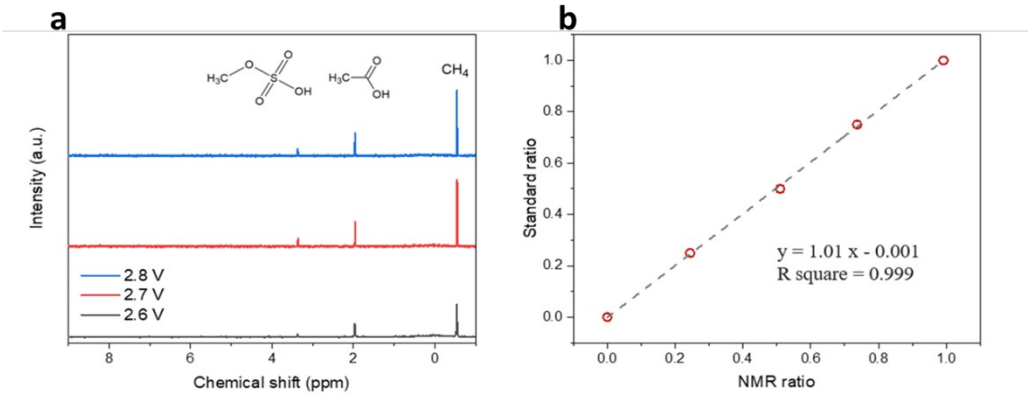

Supplementary Figure S3. a NMR result of the reaction aliquots after 6 hr electrolysis at different working potentials versus Ag/AgCl (3M KCl) reference electrode. **b** Calibration curve for the quantification of MBS using acetic acid sodium salt as the internal standard**.**

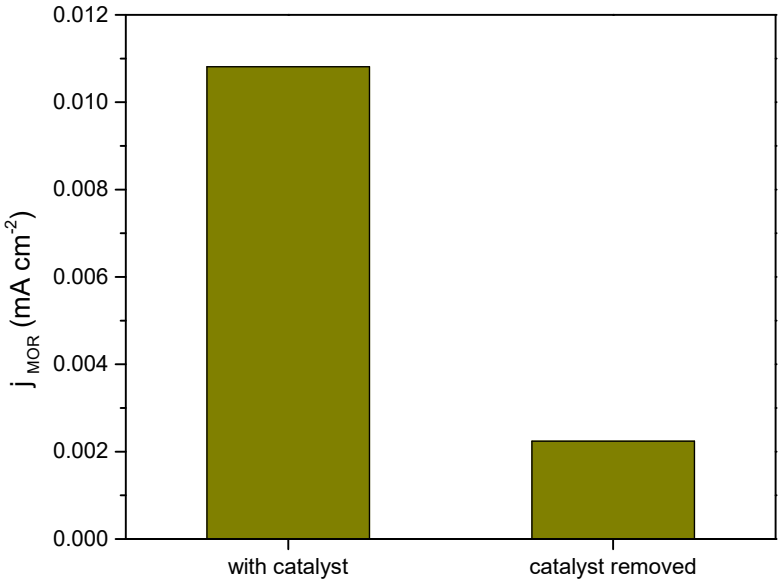

Supplementary Figure S4. Activity difference between experiments with and without the heterogeneous catalyst. Data were collected under 2.8 V vs. Ag/AgCl (3M KCl) and 1 bar methane pressure condition.

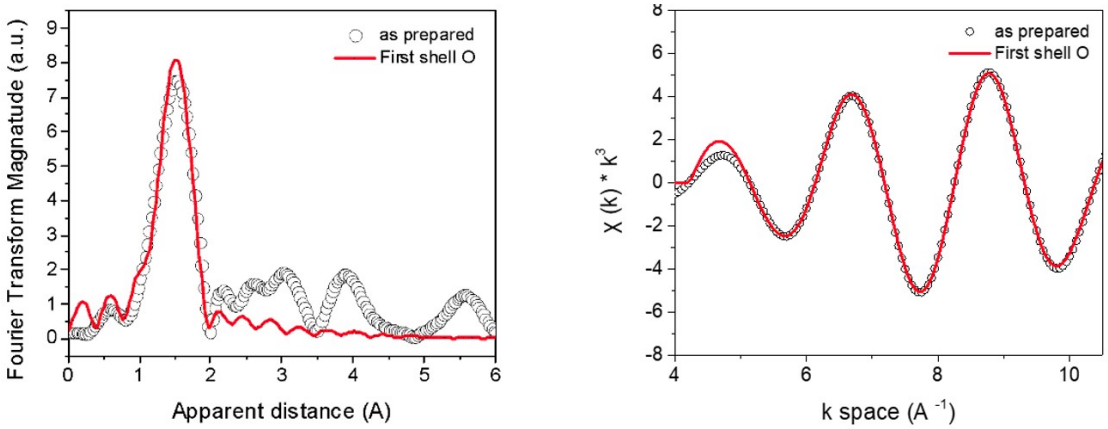

Supplementary Figure S5. Vanadium K-edge EXAFS fitting curves in R-space and k-space for vanadium phosphate nanosheet catalyst under as-prepared condition.

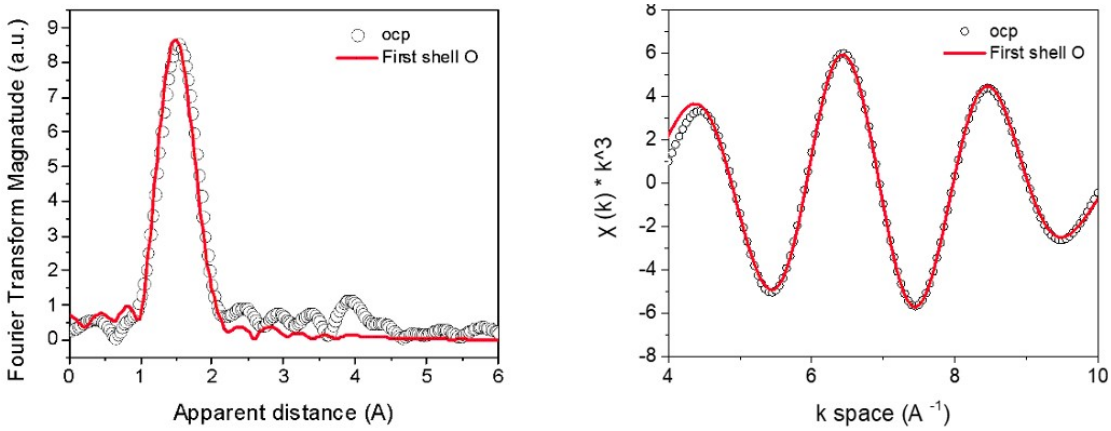

Supplementary Figure S6. Vanadium K-edge EXAFS fitting curves in R-space and k-space for vanadium phosphate nanosheet catalyst under OCP condition.

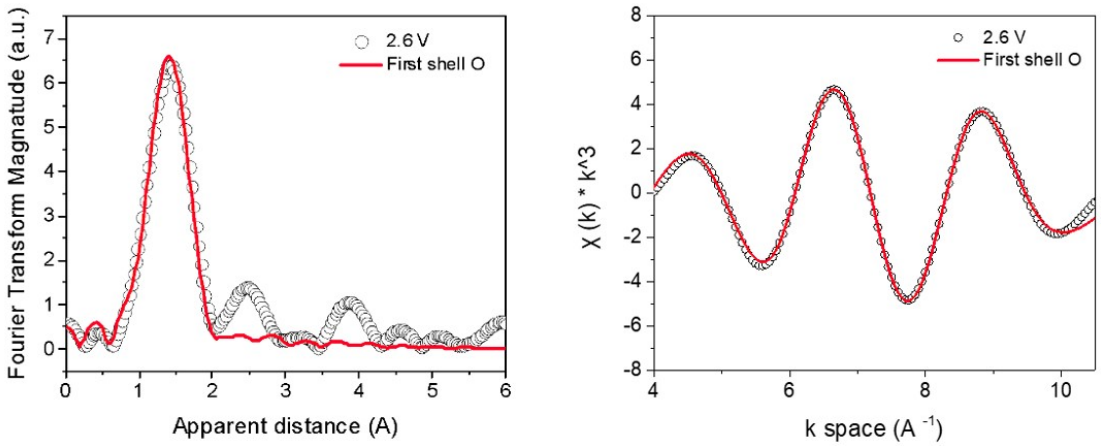

Supplementary Figure S7. Vanadium K-edge EXAFS fitting curves in R-space and k-space for vanadium phosphate nanosheet catalyst under 2.6 V (vs. Ag/AgCl) reaction condition.

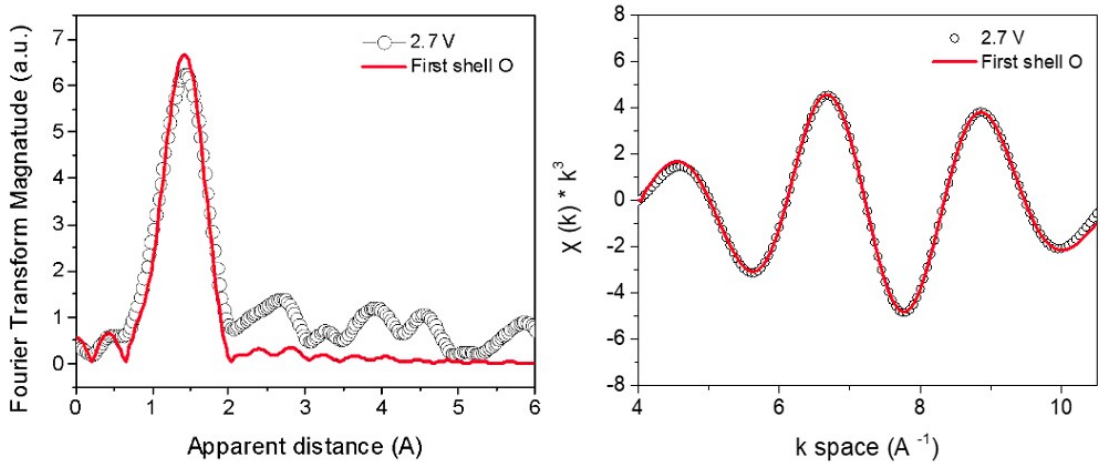

Supplementary Figure S8. Vanadium K-edge EXAFS fitting curves in R-space and k-space for vanadium phosphate nanosheet catalyst under 2.7 V (vs. Ag/AgCl) reaction condition.

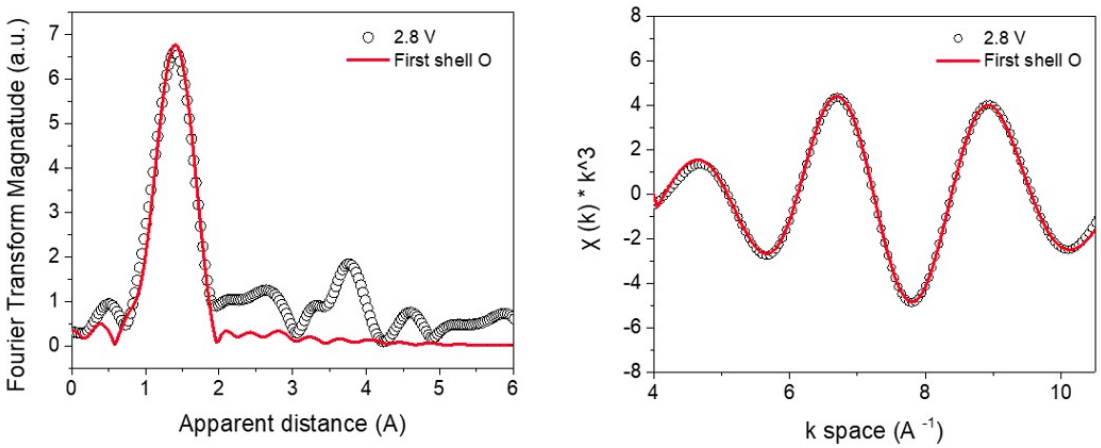

Supplementary Figure S9. Vanadium K-edge EXAFS fitting curves in R-space and k-space for vanadium phosphate nanosheet catalyst under 2.8 V (vs. Ag/AgCl) reaction condition.

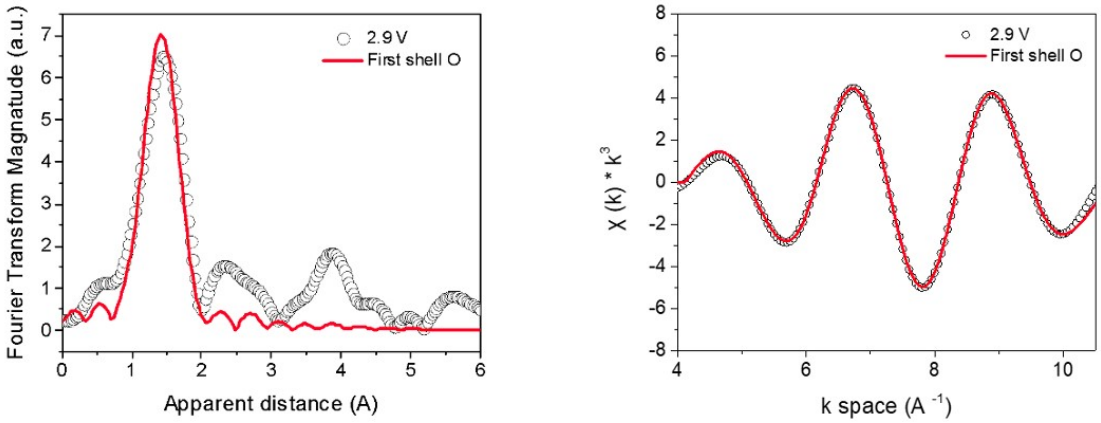

Supplementary Figure S10. Vanadium K-edge EXAFS fitting curves in R-space and k-space for vanadium phosphate nanosheet catalyst under 2.9 V (vs. Ag/AgCl) reaction condition.

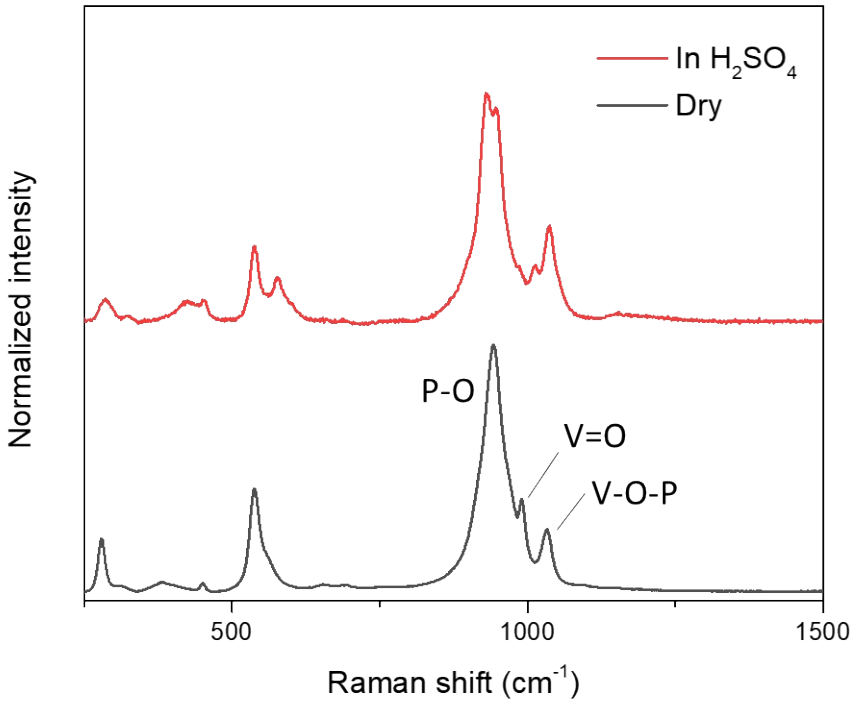

Supplementary Figure S11. Raman spectrum of the vanadium phosphate nanosheet under dry (as-prepared) and wet (OCP) conditions.

Supplementary Table S1. Entries 1,2: Experiments with the addition of 10 % SO_3, where methane sulfonic acid (MSA) was yielded instead of methyl bisulfate (MBS). Entries 3,4: Experiments with the addition of MBS conducted under argon atmosphere.

Entry	Condition	Potential (vs. Ag/AgCl, 3M KCl)	Δ Concentration (mmol hr^{-1})
1	100 % H_2SO_4 10 % SO_3 1 bar CH_4	2.8 V	Trace (MBS) 0.011 (MSA)
2	100 % H_2SO_4 10 % SO_3 1 bar CH_4	3.0 V	Trace (MBS) 0.005 (MSA)
3	98% H_2SO_4 0.22 mmol MBS 1 bar Ar	2.8 V	-9.8×10^{-6} (MBS)
4	98% H_2SO_4 0.22 mmol MBS 1 bar Ar	3.0 V	-1.7×10^{-5} (MBS)

Table S2. Comparison of the performance of different electrocatalysts in MOR.

Electrocatalyst	T (°C)	P_{CH4} (bar)	j_{CH4} (μA/cm^2)	E_a (kJ/mol)	Ref.
B-doped diamond	140	70	-	-	1
Ag_2SO_4	25	8.6	36	13.1	2
$PdSO_4$	25	34.5	-	25.9	3
Aqueous Pt^{II}	130	46.	90	-	4
Pd^{III} dimer	50	7	-	21.3	5
V-oxo dimer	25	1	50.1	10.8	6
$VOPO_4$	25	7	92.66	9.0	This work

1.

Table S3. Structural parameters from *in situ* V K-edge EXAFS during MOR.

Condition	Path*	R(Å)	CN	ΔE	σ^2(Å)	R factor
As-prepared	V-O_s	1.599 (4)	1.0 (1)	7 (2)	0.03 (2)	1.096
	V-O_e	1.934 (4)	4.0 (2)	6 (1)	0.08 (1)	
	V-O_l	2.330 (2)	1.0 (3)	9 (4)	0.08 (5)	
OCP	V-O_s	1.570 (1)	0.5 (7)	-9 (3)	0.03 (7)	1.134
	V-O_e	1.957 (4)	3.9 (2)	-6 (6)	0.07 (1)	
	V-O_l	2.400 (1)	1.7 (3)	-8 (2)	0.06 (3)	
2.6 V	V-O_s	1.532 (5)	0.8 (7)	-6 (2)	0.04 (3)	0.528
	V-O_e	1.903 (5)	4.0 (2)	-5 (8)	0.09 (1)	
	V-O_l	2.320 (1)	1.3 (2)	-5 (3)	0.08 (3)	
2.7 V	V-O_s	1.547 (5)	0.9 (8)	2 (2)	0.03 (3)	0.267
	V-O_e	1.916 (6)	4.0 (2)	1 (8)	0.10 (2)	
	V-O_l	2.320 (2)	1.2 (3)	0 (4)	0.07 (5)	
2.8 V	V-O_s	1.535 (4)	0.9 (7)	-3 (2)	0.03 (3)	0.286
	V-O_e	1.899 (5)	3.9 (2)	0 (1)	0.10 (1)	
	V-O_l	2.320 (3)	1.2 (3)	-4 (4)	0.10 (5)	
2.9 V	V-O_s	1.555 (4)	0.9 (8)	7 (2)	0.02 (3)	5.900
	V-O_e	1.911 (4)	3.9 (3)	2 (8)	0.10 (1)	
	V-O_l	2.300 (1)	1.2 (2)	-1 (3)	0.06 (4)	

* V-O_s : V-O_{short} ; V-O_e : V-$O_{equatorial}$; V-O_l : V-O_{long}

Supplementary note S1

A kinetic model is built to explain why C-H oxidation is not necessary the rate determining step despite the production rate of methyl bisulfate showing a first order dependence to the methane pressure.

A is the resting state of the catalyst, where B is the active state of the catalyst. C is methane, while D is methyl bisulfate. E is water or sulfuric acid, and F is the side products.

$$A \xrightarrow{k1} B$$
$$B + C \xrightarrow{k2} A + D$$
$$B + E \xrightarrow{k3} A + F$$

Starting condition

A (t=0) = A_0

B (t=0) = 0

C (t=0) = C_0

D (t=0) = 0

E (t=0) = E_0

F (t=0) = 0

Approximation 1: steady-state approximation

$$\frac{dA}{dt} = \frac{dB}{dt} = 0$$

$$A + B = A_0$$

$$\frac{dA}{dt} = -k_1 A + k_2 BC + k_3 BE = 0$$

$$k_1 A = (k_2 C + k_3 E) B$$

$$A = \frac{k_2 C + k_3 E}{k_1 + k_2 C + k_3 E}$$

$$B = \frac{k1}{k_1 + k_2 C + k_3 E}$$

$$\frac{dD}{dt} = k_2 BC = \frac{k_2 k_1 C}{k_1 + k_2 C + k_3 E}$$

Approximation 2: side reaction (OER) is faster than methane oxidation (MOR)

k3>k2

$$\frac{dD}{dt} = \frac{k_2 k_1 C}{k_1 + k_3 E}$$

If active site generation is the rate determining step ((k1 < k2, k3):

$$\frac{dD}{dt} = \frac{k_2 k_1 C}{k_3 E}$$

If methane oxidation is the rate determining step (k1 > k2, k3):

$$\frac{dD}{dt} = k_2 C$$

Therefore, under the existence of a fast side reaction, the production rate of MBS is linearly correlated to the concentration of methane at the electrode no matter the rate determining step is the active site formation step or the methane hydrogen subtraction step.

Reference

1. J. Britschgi, M. Bilke, W. Schuhmann and F. Schüth, *ChemElectroChem*, 2022, **9**, e202101253.
2. D. Xiang, J. A. Iñiguez, J. Deng, X. Guan, A. Martinez and C. Liu, *Angew. Chem., Int. Ed.*, 2021, **60**, 18152-18161.
3. M. E. O'Reilly, R. S. Kim, S. Oh and Y. Surendranath, *ACS Cent. Sci.*, 2017, **3**, 1174-1179.
4. R. S. Kim and Y. Surendranath, *ACS Cent. Sci.*, 2019, **5**, 1179-1186.
5. R. S. Kim, A. Nazemi, T. R. Cundari and Y. Surendranath, *ACS Catal.*, 2020, **10**, 14782-14792.
6. J. Deng, S.-C. Lin, J. Fuller, J. A. Iñiguez, D. Xiang, D. Yang, G. Chan, H. M. Chen, A. N. Alexandrova and C. Liu, *Nat. Commun.*, 2020, **11**, 3686.